LUND UNIVERSITY

Design of closely packed pattern reconfigurable antenna array for MIMO terminals

Li, Hui; Lau, Buon Kiong; He, Sailing

LUND UNIVERSITY

PO Box 117
221 00 Lund
+46 46-222 00 00

Design of Closely Packed Pattern Reconfigurable Antenna Array for MIMO Terminals

Hui Li, Buon Kiong Lau and Sailing He

Abstract—**In this paper, a compact pattern reconfigurable dual-antenna array is designed at 2.65 GHz for MIMO terminal applications, such as laptops. Each antenna is composed of two layers, i.e., the monopole layer and the PIFA layer. By switching the PIN diodes on each layer, its radiation patterns can be varied between conical and boresight patterns. Two such identical antennas are placed side by side on a common ground plane for MIMO application, providing altogether four operating modes. The center-to-center separation between the antennas is 0.25 wavelength, to keep the overall array size compact. To facilitate an isolation of above 17 dB over all modes for this compact array, two decoupling techniques based on decoupling slits and shielding wall are effectively combined. The envelope correlation coefficient (ECC) of the far-field patterns in the four modes are below 0.05 in free space, and below 0.1 for most cases in indoor and outdoor scenarios. The only exception is the monopole-PIFA mode in the outdoor scenario, but the ECC is still below 0.3 for this case. The measured efficiencies of the antennas are between -1.7 dB (68%) to -0.7 dB (85%) for all modes. Therefore, good diversity and MIMO performances are expected for the proposed design.**

Index Terms—**Antenna array, pattern diversity, reconfigurable antenna, MIMO system.**

I. INTRODUCTION

Due to its ability of increasing the data rate, multiple-input multiple-output (MIMO) is becoming a prevalent technology in modern wireless communications. However, in a multipath fading environment, the achievable capacity for the MIMO systems with fixed radiation patterns is limited by the fast-changing channels. One solution is to adapt the radiation patterns of the antennas to the environment, which has been reported to effectively increase the channel capacity [1], [2].

Pattern reconfigurable antennas have been intensely studied in recent years, e.g., [3]-[12]. A commonly used design is the electrically steerable passive array radiator (ESPAR), which includes one driven element in the center and several parasitic elements around the driven element [6], [7]. It has been used for MIMO applications and has been reported to improve the average channel capacity by 37% [7]. However, the size of ESPAR antenna and the required distance between the elements render it unsuitable for terminal applications. Thus,

planar reconfigurable MIMO arrays were proposed [9]-[12]. The pattern reconfigurable antenna in [9] was applied to a mobile handset, with the far-field pattern of each antenna varying between that of loop and dipole antennas. The two antennas were orthogonally placed along the shorter and longer edges of the chassis, respectively. In [10], 8 PIN diodes were used to change the radiation patterns of the U-slot etched patch antenna between the normal patch pattern and the monopole pattern. The dual-antenna setup was successfully measured for capacity improvement. Piazza *et al.* proposed a circular patch for pattern reconfiguration using different radiation modes of the patch, with a single element size of 0.37 wavelength (λ) [11]. Similarly, an Alford Loop design with boresight and monopole patterns was introduced in [12]. In the abovementioned cases, to keep the correlation of the antennas at a low level for all the reconfigurable modes, the distance between the antenna elements was at least 0.47λ.

In this paper, a compact pattern reconfigurable array, with single element size of $\lambda/6 \times \lambda/6$ and an edge-to-edge distance of $\lambda/11$, is proposed for terminal application such as laptops. The antenna is based on planar inverted-F antenna (PIFA) structure, so that the dimension can be reduced by half compared with patch- or dipole-based reconfigurable antennas. The PIFA structure provides the boresight pattern, whereas the conical pattern is attained when a capacitively coupled plate is connected to the PIFA, forming a top-loaded monopole. For MIMO application, to reduce the distance between two antenna elements, the decoupling structures of defected ground plane and shielding wall are combined to reduce mutual coupling for all operating modes. The reconfigurable array provides four different modes with relatively balanced power. The envelope correlation coefficients (ECCs) between the two antennas in all four modes is below 0.05 in free space.

II. SINGLE ANTENNA DESIGN

The proposed pattern reconfigurable antenna is shown in Fig. 1. The antenna consists of a monopole layer and a PIFA layer. The monopole layer (see Fig. 1(b)) has a square patch and a via connected with the ground plane. A PIN diode (i.e., switch 1) is added between the via and the patch.

In the PIFA layer, a slot is etched, where two PIN diodes (i.e., switch 2) are applied to change the connection status between the patch and the shorting wall. A square hole is etched around the location of the via in the PIFA layer to make sure that the monopole layer and the PIFA layer are not physically connected. A substrate (F4BM350) with a thickness of 0.5 mm, a permittivity of 3.48 and a loss tangent of 0.003 is added between the two layers. The same substrate is also applied on the ground plane for the convenience of antenna implementation. The size of the ground plane is 50 mm × 50 mm. The detailed dimensions of the structure are shown in the caption of Fig. 1. The relative positions of the PIN diodes are illustrated in Fig. 4(b).

The feed of the antenna is on the PIFA layer. When switch 1 is on and switch 2 is off, the antenna feed induces current on the lower patch (PIFA layer). Due to the coupling effect of the parallel plate, current then flows along the upper patch

(monopole layer). The upper patch and the via together forms a capacitively loaded monopole antenna with small electrical size. When switch 1 is on and switch 2 is off, the shorting wall is connected, and the PIFA mode is activated. By careful optimization, the two modes work at the same frequency band.
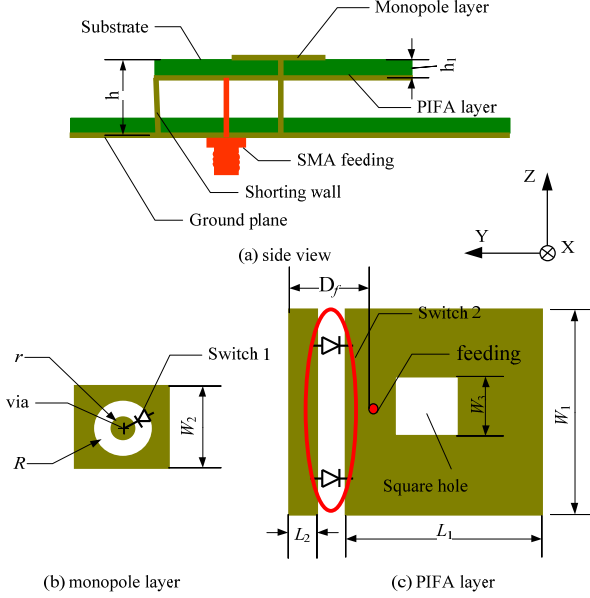

Fig. 1. The geometry of the proposed pattern reconfigurable antenna. (a) side view; (b) monopole layer; (c) PIFA layer. The dimensions are: $L_1 = 16.3$ mm, $L_2 = 2$ mm, $W_1 = 19.3$ mm, $W_2 = 5.1$ mm, $W_3 = 4.2$ mm, $r = 0.75$ mm, $R = 1.45$ mm, $h = 7$ mm, $h_1 = 0.5$ mm, $D_f = 5.8$ mm.
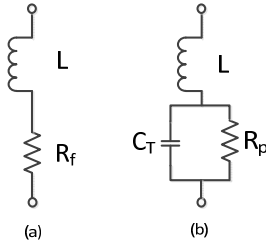

Fig. 2. Equivalent circuit for PIN diode (a) forward bias (b) reverse bias. $R_f = 0.45$ Ω, $C_T = 0.85$ pF, $R_p = 100$ kΩ, $L \approx 0$ (short wire).
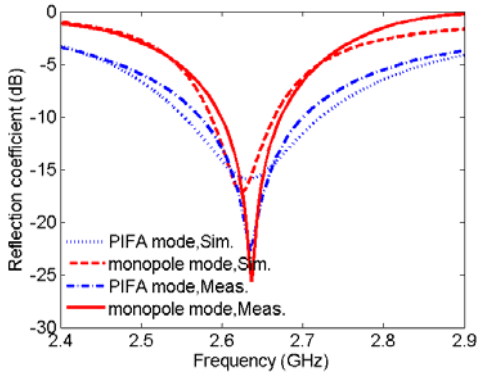

Fig. 3. Comparison of simulated and measured S-parameters of the prototype

PIN diodes from Infineon (BA892) are used to reconfigure the antenna. The equivalent circuit of the PIN diode and its values are shown in Fig. 2. The inductance L is very small due to the wire being short, and thus it is neglected in the simulation.

The antenna is simulated in the time-domain solver using CST Microwave Studio. The simulated and measured reflection coefficients of the proposed antenna after optimization are shown in Fig. 3. The center frequency of the reconfigurable antenna is 2.62 GHz, with the PIFA mode covering 2.55-2.73 GHz and monopole mode covering 2.57-2.665 GHz. The overlap bandwidth measured at 10 dB is 96 MHz. The bandwidth of the monopole is relatively narrow due to its small height of 7 mm ($\lambda/15$).

III. PATTERN RECONFIGURABLE ANTENNA ARRAY

A. Antenna Setup

To allow for the possibility of placing more than two antennas in the array, the antenna elements are placed in the same orientation, rather than symmetrically (back-to-back) on the ground plane, as shown in Fig. 4. The dimension of the ground plane is slightly enlarged to 50 mm × 70 mm, and the distance between the antennas is 10 mm, corresponding to $\lambda/11$. The status of the switches and their corresponding operating modes, i.e., PP (PIFA-PIFA) mode, PM (PIFA-monopole) mode, MP (monopole-PIFA) mode and MM (monopole-monopole) mode, are described in Table I.

TABLE I
OPERATING MODES AND SWITCH STATUS

	Antenna 1		Antenna 2	
	Switch 1	Switch 2	Switch 1	Switch 2
PP mode	off	on	off	on
PM mode	off	on	on	off
MP mode	on	off	off	on
MM mode	on	off	on	off
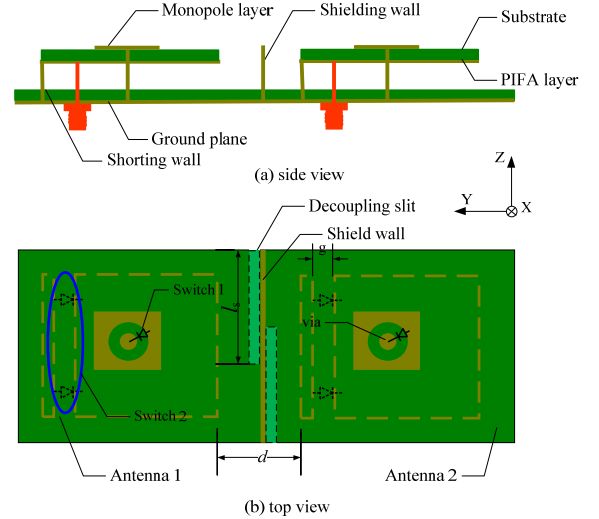
Fig. 4. Geometry of the proposed pattern reconfigurable antenna array. (a) side view; (b) top view. The dimensions are: $d = 10$ mm, $g = 1$ mm.

B. Decoupling Techniques

Coupling coefficient and ECC are critical parameters for MIMO antennas. In order to keep them at a low level, the antennas are normally spaced far away from each other [8]-[12]. In order to reduce the distance while keeping mutual coupling at a low level, a combination of decoupling techniques is proposed for the antenna array, i.e., the decoupling slits and the

shielding wall. Though the decoupling slits and shielding walls are not new techniques, they had only been considered separately in the existing literatures. In this work, we use the combination of the two techniques in a very limited volume to effectively provide 4-5 dB additional isolation, in comparison to the use of a single technique. Firstly, two quarter wavelength slits are etched from different sides of the ground plane between the two antennas, as shown in Fig. 4(b). The slits work as a band-stop filter with the stopband at around 2.6 GHz, leading to low transmission coefficients between the two ports [14], [15]. However, due to the limited spacing (d), not more than two slits can be used, and thus its effect is limited. To efficiently reduce the mutual coupling for all reconfigurable modes, a shielding wall with the same height as the antenna is employed in between the slits, which operates as a reflector and slightly redirects the radiation patterns of the antennas. The changing of the radiation patterns by the shielding wall is studied in Table II. We only show the results for antenna 1, as a similar effect is observed for antenna 2. It can be seen from the figure that the radiation pattern without the shielding wall is already tilted due to the existence of the other antenna as reflector and scatterer. With the shielding wall, the radiation patterns become more directive as a result of the reflection from the wall. The only exception is the antenna in the MP mode, where the radiation pattern is similar with and without the wall. This is because the PIFA, as the second antenna, has a shorting wall by itself, which functions similarly as the shielding wall. On the other hand, the slits are more effective for the monopole than for PIFA in reducing mutual coupling, as seen in Table III.

To investigate the effectiveness of each decoupling structure, S-parameters of the antenna array are simulated with one decoupling structure applied at each time. As representative cases, the simulation results of the S-parameters in the PP and MM modes are shown in Figs. 5(a) and 5(b). As a reference, the initial isolation between the MIMO antennas without any decoupling structures is around 7 dB and 8 dB for the PP and MM modes, respectively. The S-parameters for the case without decoupling techniques are omitted for clarity of the figures. In the PP mode, it is observed the decoupling slits and the shielding wall are both effective in reducing the coupling, with the isolation improved to 10 dB using each technique. When the two decoupling structures are employed together, an isolation of above 17 dB is achieved, whereas the reflection coefficients of both antennas are almost unchanged. For the MM case, the decoupling slit is more effective than the shielding wall, enhancing the isolation to 13 dB by itself (as opposed to around 10 dB using only the shielding wall).

The effects of each structure on ECC, coupling coefficient and total efficiency are presented in Table III. It is observed that the correlation is sufficient low in all cases for MIMO performance, and it is further reduced by the decoupling structures, especially by the slits in the ground plane. The main contribution of the decoupling structure is to decrease the coupling coefficient, and thus increase the total efficiency of the antennas. The decoupling slits can increase the efficiency of the antennas by around 4%. The combination of the two decoupling structures provides a 7% and 5% increase in

efficiency for the PP and MM modes, respectively. It should be noted that though the variation of the efficiency is mainly attributed to the mutual coupling, the impedance matching at the port also has slight effect.

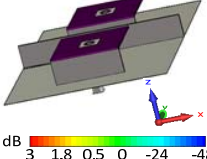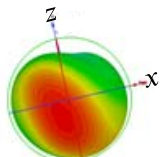TABLE II
INFLUENCE OF SHIELDING WALL ON RADIATION PATTERN
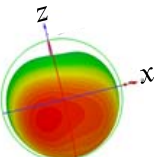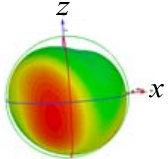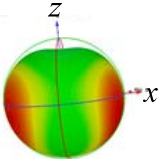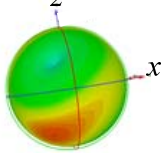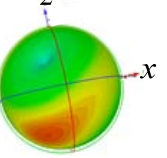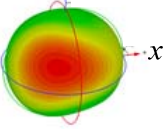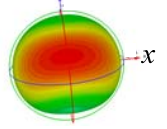
TABLE III
INFLUENCE OF DECOUPLING STRUCTURES ON ECC, COUPLING
COEFFICENT AND TOTAL EFFICIENCY

	ECC		Coupling coefficient		Total efficiency			
	PP mode	MM mode	PP mode	MM Mode	PP mode		MM mode	
Original	0.21	0.14	-7 dB	-8 dB	85.8%	86.7%	79.5%	79.2%
Slits only	0.08	0.09	-10dB	-13 dB	90.6%	90.1%	82.2%	80.9%
Wall only	0.19	0.1	-10dB	-10 dB	89.8%	90.2%	81.4%	80.8%
Slits&Wall	0.001	0.02	-17dB	-17 dB	92.3%	93.2%	84.7%	82.2%

(a)

(b)
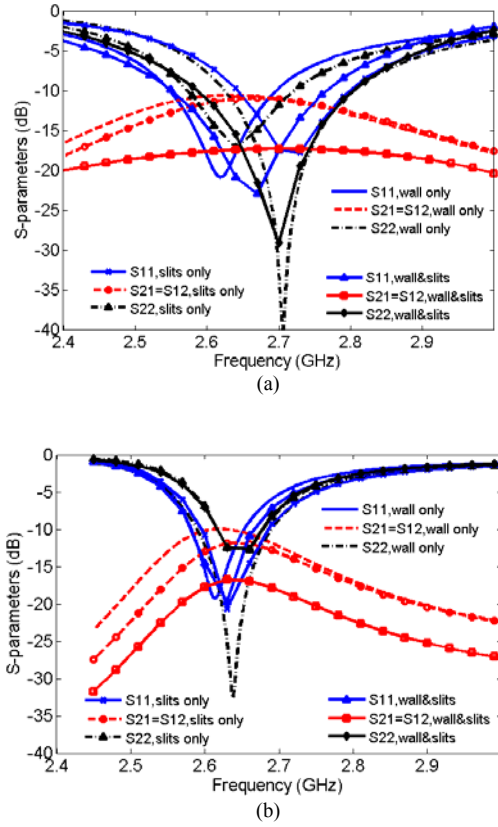
Fig. 5. The S-parameters of the antenna array with the decoupling slits, the shielding wall, or both: (a) PP mode and (b) MM mode.

It is worth noting that the proposed combination of the decoupling structures can be used in general to further improve the isolation of compact MIMO antennas. Importantly, for reconfigurable MIMO antennas, the combination of the two techniques can provide effective decoupling over different operating modes.

IV. EXPERIMENTS AND DISCUSSIONS

The prototype of the reconfigurable MIMO antenna was fabricated, as shown in Fig. 6. In the experiment, the status of the PIN diodes was controlled by the voltage applied, which was provided by a 3V lithium battery. The bias circuit, composed of a RF choke inductor (L_R), a DC blocking capacitor (C) and a resistor (R), is shown in Fig. 7. The resistor R is used to set the forward current for the PIN diode to around 10 mA, leading to an equivalent forward resistance of 0.4 Ω according to the current-resistance curve in the data sheet. The shorting wall and the shorting PIN in the center are connected to the ground plane, respectively, in the PIFA and monopole mode, so it is ensured that one end of the PIN diode is connected to ground plane as shown in Fig. 7. In the prototype, the battery and the resistance (R) of the bias circuit were put underneath the ground plane to reduce their disturbance on the antennas' operating frequency and radiation. The RF choke (L_R) and the DC block (C) were placed near the PIN diode.

Due to the fabrication tolerance and the non-ideal performance of the PIN diodes, the resonant frequency of the

PIFA was shifted to a lower frequency. To tune the resonance back, another PIN diode is added to switch 2. Two of the PIN diodes are located at the open edge, while the third PIN diode is at the center of the slit. The final measured S-parameters of the proposed antenna array at the four operating modes are shown in Fig. 8. The center frequency of the reconfigurable antenna is 2.65 GHz. Similar as the single antenna case, the worst bandwidth of around 92 MHz is limited mainly by the monopole mode.
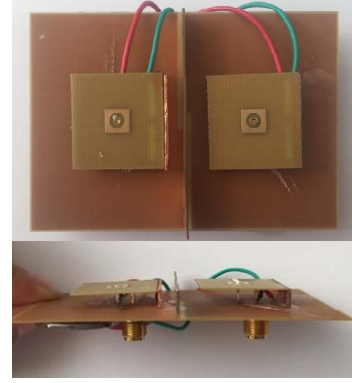
Fig. 6. Fabricated prototype of the proposed reconfigurable MIMO array.
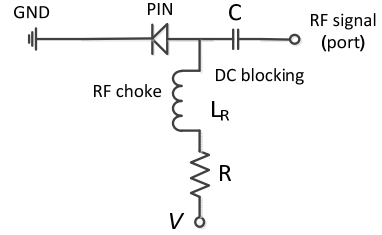
Fig. 7 Biasing circuit of the PIN diode. R = 300 Ω, C = 220 pF, L_R = 100nH.
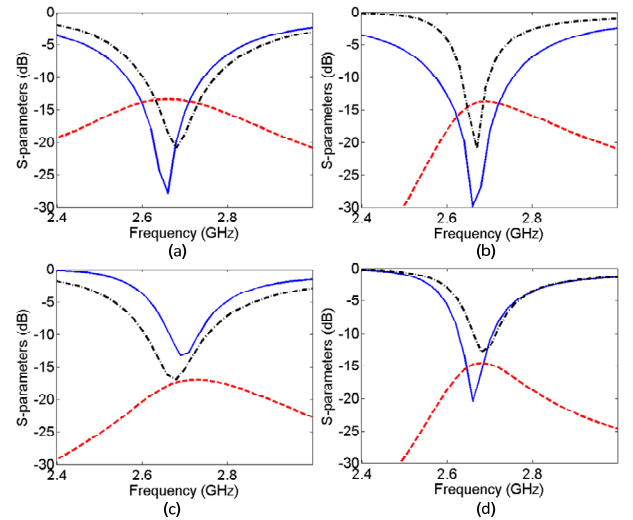
Fig. 8. Measured S-parameters of the proposed antenna array in (a) PP mode, (b) PM mode, (c) MP mode and (d) MM mode.

Antenna patterns and efficiencies were measured in a Satimo antenna measurement facility. For each operating mode, the battery is connected to or disconnected from the circuit according to the on/off status of the PIN diodes in Table I.

During the pattern measurement, one port is excited and the other port is terminated with a 50 ohm load. Figure 9 provides the simulated and measured patterns of the proposed antenna array at 2.65 GHz, which shows good agreement with each other. Due to the finite modified ground plane and the existence of the other antenna, the final radiation patterns are more diverse than the typical conical and boresight patterns of a single element. When the array operates in the PP mode, the radiation pattern in both *xoz* and *yoz* planes points upward and downward for port 1 and port 2, respectively. This is because strong current is distributed along both slots when port 1 is excited. The radiation of the slots contributes greatly to the downward pattern. On the other hand, due to the shorting wall of the PIFA preventing the current from flowing to the slots, the current is significantly lower along the slots when port 2 is excited. In the PM mode, the radiation pattern of antenna 1 does not change much compared with the PP mode, whereas antenna 2 presents a monopole-like radiation pattern, with its nulls in 0° and 180°. The small differences between the simulated and measured patterns could be due to the existence of the bias circuit and battery not modeled in the simulations. In the *xoy* plane, antenna 1 and 2 radiate maximum powers towards 70° and 250°, respectively. In the MP mode, the radiation pattern of the monopole mode is tilted to 30° and 210°, mainly owing to the shielding wall. Comparing with the PP mode, it is noticed that though antenna 2 operates as a PIFA in both modes, the radiation patterns are largely different due to the different loadings of antenna 1. The phenomenon is also true for the other cases. This offers more diverse radiation patterns. In the MM mode, the maximum radiation points to 300° and 90°, respectively, in *yoz* plane for antenna 1 and 2. In *xoz* plane, antenna 1 is omni-directional.

From practical perspective, apart from maximizing received signal power, MIMO systems can also benefit from pattern reconfiguration through interference mitigation. For example, if the desired signal is from the endfire direction, whereas the interference is from boresight, the PM mode can be used for spatial multiplexing; If the interference is from 300 degree to 330 degrees, either antenna 1 in the MM mode or antenna 2 in the PM mode can be utilized, depending on the arrival angle of the signal. This way, the signal-to-interference plus noise ratio (SINR) can be increased, leading to a more reliable link.

The measured total efficiencies of the array elements for different modes at 2.65 GHz are presented in Table IV. Compared with the simulation results in Table III, the measured efficiencies are around 0.5 dB lower for the PIFA, whereas it is around 1 dB for the monopole antenna. These small discrepancies can be attributed to pattern measurement and fabrication tolerances, as well as the insertion loss of the PIN diodes (0.2 dB from the data sheet) and the biasing circuit.

In the four operating modes, the efficiencies of the monopole (M) mode are lower than that of the PIFA (P) mode by around 1 dB, due to the substrate loss at the coupled feed and insertion loss of the PIN diodes. The largest power imbalance between the branches is around 1 dB, which can be compensated by waterfilling and MRC (Maximum Ratio Combining) algorithm for better capacity and diversity performance, respectively.
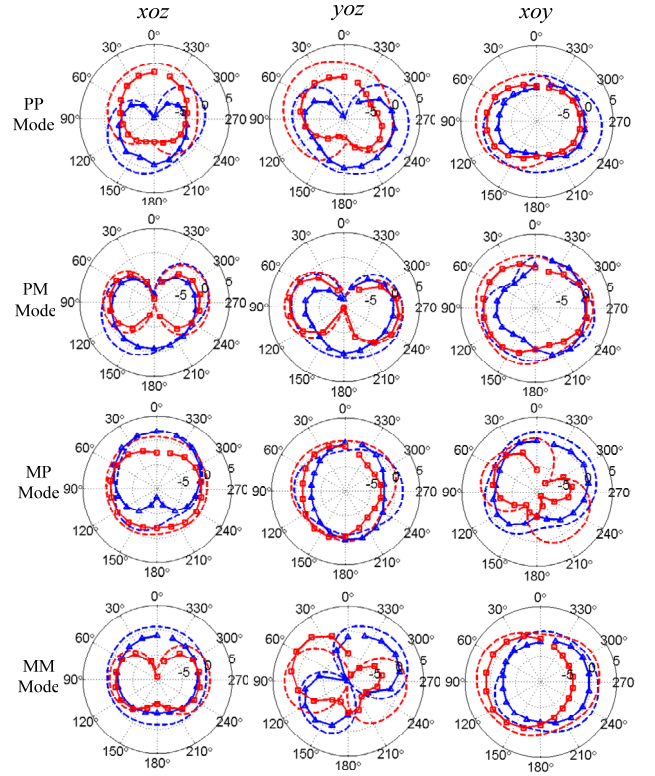

Fig. 9. Radiation patterns (in realized gain) of the proposed antenna array at 2.65 GHz: (– –) antenna 1, simulated; (–△–) antenna 1, measured; (– –) antenna 2, simulated, (–☐–) antenna 2, measured.

TABLE IV
MEASURED TOTAL EFFICIENCIES OF THE MIMO ARRAY

	Port 1	Port 2
PP mode	85% (-0.68 dB)	82% (-0.86 dB)
PM mode	84% (-0.75 dB)	68% (-1.7 dB)
MP mode	69% (-1.61 dB)	78% (-1.36 dB)
MM mode	74% (-1.34 dB)	75% (-1.25 dB)

The ECC of the proposed antenna array is investigated for the four modes and three different propagation scenarios, i.e., an ideal scenario with isotropic angular power spectrum (APS), an indoor scenario and an outdoor scenario. For terminal application, a uniform APS distribution is a reasonable assumption for the azimuthal plane, as was assumed in [16]. For the elevation plane, Gaussian and Laplacian APS distributions are assumed for the indoor and outdoor scenarios, respectively. The parameters for the indoor and outdoor scenarios, similar to those in [17], are given in Table V. In Table V, m_v and m_h are the mean elevation angles of vertical and horizontal polarized wave distributions, respectively. σ_v and σ_h are the standard deviations of the vertical and horizontal polarized wave distributions, respectively.

The ECCs over frequency for the four modes are shown in Fig. 10. In the isotropic scenario, the ECCs are below 0.05 at the operating frequencies. For the indoor and outdoor scenarios, the ECCs are quite low (below 0.1) in general, except for the MP mode in the outdoor scenario, which has a maximum ECC of 0.3 at 2.6 GHz. However, the highest ECC is still far below the criteria of 0.5 [18]. In practice, priority can be given to the other three modes, to guarantee the lowest possible ECC.

TABLE V
PARAMETERS FOR INDOOR AND OUTDOOR SCENARIOS

	m_v	m_h	σ_v	σ_h	XPR
Indoor	20°	20°	30°	30°	1 dB
outdoor	10°	10°	15°	15°	5 dB

TABLE VI
COMPARISON WITH THE STATE-OF-ART ANTENNAS

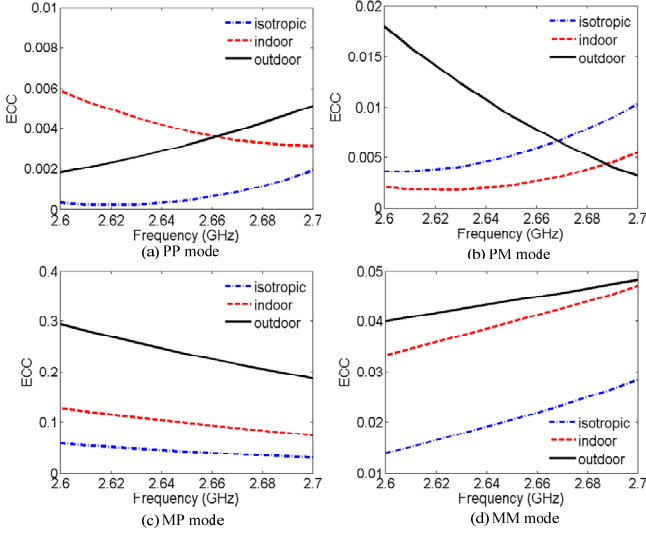|	Type	Com-plexity	Size of single antenna	Distance between antennas	S_{21}	ECC (free space)	Meas. Eff.	BW
Ref. [9]	Loop & Dipole	Low	$\frac{\lambda}{4} \times \frac{\lambda}{4}$	0.47λ	<-20 dB	< 0.03	70%-79%	3.8%
Ref. [10]	Patch based	Me-dium	$\frac{\lambda}{3} \times \frac{\lambda}{3}$	λ	<-20 dB	< 0.04	45%-87%	6.6%
Ref. [12]	Alford loop	Low	$\frac{\lambda}{2} \times \frac{\lambda}{2}$	0.5λ	<-14.5 dB	-	-	9.8%
Proposed	PIFA based	Me-dium	$\frac{\lambda}{6} \times \frac{\lambda}{6}$	0.25λ	<-15 dB	< 0.05	68%-85%	3.8%

Fig. 10. ECC for isotropic, indoor and outdoor scenarios.

The proposed antenna is compared with the state-of-art reconfigurable MIMO arrays in terms of size, complexity, coupling coefficient (S_{21}), efficiency, bandwidth and type, as shown in Table VI. All the antennas in comparison can redirect their patterns between conical and boresight patterns. It is seen that both the single element size and the distance between the elements of the proposed antenna is much smaller than the other prototypes. The coupling coefficient and ECC of all the antennas are at similar levels. At the same time, the measured efficiencies of the proposed antenna are more balanced than that in [10], meaning a more balanced power. The main drawback of the proposed antenna is its implementation complexity and relatively small bandwidth due to its top loaded structure.

V. CONCLUSION

In this paper, a closely packed pattern reconfigurable antenna array was proposed for MIMO terminals, such as laptops. Each of the two antenna elements can be switched to provide either a conical pattern or a boresight pattern. With two antennas placed side by side, four operating modes were achieved. A combination of decoupling slits and the shielding wall was constructed between the antenna elements to provide an isolation of over 17 dB for all the four operating modes. The distance between the antennas is $\lambda/11$, allowing a compact implementation. The correlations between the two antennas are low for the ideal isotropic, indoor and outdoor scenarios in all four operating modes. Compared with other MIMO reconfigurable antennas, the proposed array performs well in terms of having a smaller size while having similar antenna performances.

REFERENCES

[1] M. Fernandez, et al., "Spectral efficiency in MIMO systems using space and pattern diversities under compactness constrains," *IEEE Trans. Veh. Technol.*, vol. 57, no. 3, pp. 1637-1645, May 2008.

[2] P. Qin, T. J. Guo, and E. Dutkiewicz, "Capacity enhancement of 2 × 2 MIMO system using pattern reconfigurable antennas," in *Proc. Asia-Pacific Microw. Conf. (APMC)*, Melbourne, Australia, Dec. 5-8, 2011, pp.1694-1697.

[3] E. R. Iglesias, O. Quevedo-Teruel, and M. S. Fernandez, "Compact multimode patch antennas for MIMO applications," *IEEE Antennas Propag. Mag.*, vol. 50, no. 2, pp. 197-205, Apr. 2008.

[4] T. Aboufoul, C. Parini, X. Chen, and A. Alomainy, "Pattern-reconfigurable planar circular ultra-wideband monopole antenna," *IEEE Trans. Antennas Propag.*, vol. 61, no. 10, pp. 4973-4980, Oct. 2013

[5] C. Christodoulou, Y. Tawk, S. Lane, and S. Erwin, "Reconfigurable antenna for wireless and space applications," *Proc. IEEE*, vol. 100, no. 7, pp. 2250-2261, Jul. 2012.

[6] Z. H. Hu, P. S. Hall, and P. Gardner, "Reconfigurable dipole-chassis antennas for small terminal MIMO applications," *IET Electron. Lett.*, vol. 47, no. 17, Aug. 2011.

[7] H. Liu, S. Gao, and T. H. Loh, "Compact MIMO antenna with frequency reconfigurability and adaptive radiation patterns," *IEEE Wireless Antenna Propag. Lett.*, vol. 12, pp. 269-272, 2013.

[8] Y. Zhou, R. Ave and S. Hum, "Design and evaluation of pattern reconfigurable antennas for MIMO applications," *IEEE Trans. Antennas Propag.*, vol. 62, no. 3, pp. 1084-1092, Mar. 2014.

[9] C. Rhee, et al., "Pattern reconfigurable MIMO antenna for high isolation and low correlation," *IEEE Wireless Antenna Propag. Lett.*, vol. 13, pp. 1373-1376, 2014.

[10] P. Qin, Y. Guo, A. Weily, and C. Liang, "A pattern reconfigurable antennas U-slot antenna and its applications in MIMO systems," *IEEE Trans. Antennas Propag.*, vol. 60, no. 2, pp. 516-528, Feb. 2012.

[11] D. Piazza, et al., "Stacked reconfigurable circular patch antenna for adaptive MIMO systems," *in Proc. Int. Conf. Electromagn. Advanced Applic. (ICEAA)*, Torino, Sep. 2009, pp. 636-639.

[12] D. Patron, K. R. Dandekar, and D. Piazza, "A reconfigurable antenna with omnidirectional and directional patterns for MIMO systems," in *Proc. IEEE Antennas Propag. Soc. Int. Symp. (APS)*, Orlando, FL, Jul. 7-13, 2013, pp. 204-205.

[13] H. Li and S. He, "A compact reconfigurable antenna with pattern diversity," *IEEE Int. Symp. Antennas Propag., Chicago*, IL, Jul. 2012.

[14] H. Li, J. Xiong, and S. He, "A compact MIMO antenns system of four elements with similar radiation characteristics and isolation structure," *IEEE Antennas Wireless Propag. Lett.*, vol. 8, pp. 1107-1110, 2009.

[15] H. Li, J. Xiong, Z. Ying, and S. He, "High isolation compact four-port MIMO antenna systems with built-in filters as isolation structure," *in Proc. 4th Europ. Conf. Antennas Propag.*, Barcelona, Spain, Apr. 2010

[16] T. Taga, "Analysis of mean effective gain of mobile antennas in land mobile radio environments," *IEEE Trans. on Vehicular Technology,* vol. 39, no. 2, pp. 117-131, May 1990.

[17] Z. Ying and V. Plicanic, "Characterization of multi-channel antenna performance for mobile terminal by using near field and far field parameters," in *COST 273 TD(04) 095*, Goteborg, Sweden, Jun. 2004.

[18] R. G. Vaughan and J. B. Andersen, "Antenna diversity in mobile communications," *IEEE Trans. Veh. Technol.*, vol. 36, no. 4, pp. 149–172, 1987.